Delineation of the Aquifer in the Curin Basin, South of Zahedan City, Iran

[1]Hadi Tahmasbi Nejad, [2]Fatemeh Zakeri Hoseini, [1]Mehdi Mumipour, [1]Abdolreza Kaboli and [1]Morteza Najib
[1]Department of Geology, Behbahan Branch, Islamic Azad University, Behbahan, Iran
[2]Department of Geology, Khuzestan Water and Power Authority
Keywords: Vertical electrical sounding (VES), Interpretation, Curin aquifer.

Abstract
Resistivity method using 596 Schlumberger vertical electrical soundings along 26 profiles are conducted in the Curin basin, Iran to investigate the sub-surface layering and aquifer characteristics. The results of quantitative and qualitative interpretation of data reveal four layers. The true resistivity of the top soil varies from 3 to 800 ohm-m while the thickness varies from 0.5-15 m. The second layer (dry alluvium) is thicker than the surface layer with resistivity values less than 100 ohm-m. The third layer, which constitutes an aquifer, has resistivity values of less than 10 ohm-m and depth values of less than 30 m in most locations. The maximum depth of aquifer is 60 meters in the northwest and southeast portion of the study area. The fourth layer (bedrock) is characterized by two electric resistivity values ranges. In most parts of the area, it is more than 60 ohm-m, corresponding probably to slate, while in other areas, it is less than 60 ohm-m, corresponding probably to shale. Finally from the quantitative interpretation of VES curves, the limits of the aquifer were determined.

Introduction
The technique of vertical electrical soundings using a Schlumberger array, consists of a fast and versatile procedure of geophysical investigation. This method, a low-cost technique, is suitable for hydrogeological surveys of sedimentary basins and is commonly used for surveying for water in arid areas [1]. It is well known that this method can be successfully employed for ground water investigations, where a good electrical resistivity contrast exists between the saturated and unsaturated layers. This method is regularly used to solve a wide variety of groundwater problems. Some recent studies include: determination of zones with high yield potential in an aquifer [2 – 5], determination of the boundary between saline and fresh water zones [6 – 8], delineation of groundwater contamination [9 -11], exploration of geothermal reservoirs [12, 13], groundwater exploration in hard rock [14 -16], estimation of aquifer specific yield [17] and estimation of hydraulic conductivity and transmissivity of aquifer [18 – 21].

This study was conducted in an arid region in the Curin basin. It is located south of Zahedan, in the southeastern part of Iran (Fig. 1). Specifically, the study lies between latitude 28° 47' and 29° 00' north and longitude 60° 13' to 60° 29' east, covering an area of about 800 km^2. The study area has a terrain elevation average 1500 m and its climate is desertic and arid, with the annual temperature ranging between 8 and 42°C. The average annual rainfall is around 73 mm.

Material and Methodology
The resistivity technique examines horizontal and vertical discontinuities in the electrical

properties of the ground. It measures earth resistivity by passing an electrical current into the ground and measuring the resulting potentials created. This method involves the supply of direct current or low-frequency alternating current into the ground through a pair of electrodes and the measurement of the resulting potential through another pair of electrodes (potential electrodes) [22]. Because the current is known and the potential can be measured an apparent resistivity can be calculated. The apparent resistivity of the subsurface material is a function of the magnitude of the current, the recorded potential difference and the geometry of the electrode array used. The current electrodes spacing (AB) increases after each reading while the potential electrodes spacing (MN) increases only when deemed necessary and controlled by the relation $AB/2 \geq 5MN/2$ as required by the Schlumberger array [23]. For Schlumberger soundings (Fig. 2a), the apparent resistivity values (ρ_a) were plotted against half current electrode separation (AB/2) on a log-log graph and a smooth curve was drawn for each of the soundings (Fig. 2b). Then, the sounding curves were interpreted to determine the true resistivities and thicknesses of the subsurface layers. The depth of penetration is proportional with the Schlumberger array (Fig. 2c) to the separation of the current electrodes and is increased in order to penetrate deeper into the earth. However, the relationship between separation and depth is a function of the electrical structure. In general, the depth of penetration is small with this method, and only shallow subsurface layers have been surveyed [24].

Aquifer resistivity is controlled by water content, water quality and grain matrix (including shape, diameter and sorting of the grains, geometric packing arrangement and degree of matrix cementation) [5]. Rock resistivity depends on a number of factors such as the amount of water present in fractures, weathering, porosity, fracturing and the degree of saturation [25].With decreasing grain-size and water quality, the resistivity value is decreased. In saturated layers having high resistivity water and small-grain size, the electrical current is not only conducted by the water but also by the grain matrix [26].

A total number of 596 vertical electrical soundings (VES) with a spacing of 750 meters were conducted along 26 geoelectric profiles, in order to evaluate the geoelectrical setting of the Curin basin, south of Zahedan, Iran (Fig. 1). The soundings are arranged along profiles ranging approximately east-west. The profiles were spaced 1000m from each other. The VES data were acquired using a KD Sound Terrameter instrument with current electrode separation (AB) varying from 2 m up to 1000 m in successive steps.

The apparent resistivity data are associated with varying depths relative to the distance between the current and potential electrodes and can be interpreted qualitatively and quantitatively in terms of a lithologic and/or geohydrologic model. In the qualitative interpretation method the shape of the field curve is observed to assess the number of layers and their resistivity. The results of this method yield isoapparent electrical resistivity maps and geoelectrical pseudosections. In the quantitative interpretation method true resistivity ‘ρ’ and layer thickness ‘h’ as the fundamental characteristics of a geoelectric layer are obtained. The results of this method are represented in the form of the resistivity values that can be used for preparing an isoapparent electric resistivity map and the geoelectric cross-sections. These cross-sections reflect both lateral and vertical variations in resistivity. The quantitative interpretation of VES curves in this study was done by the well–known method of curves matching. In curves matching technique, the field VES curves are compared with set of theoretical curves to obtain ‘ρ’ and ‘h’. To procure initial model parameters the field curve is matched with standard curves and also by auxiliary point technique [27]. It is anticipated that the results of this study could also be used to determine the aquifer boundary of the study area.

Results and discussion

Isoapparent resistivity maps

The isoapparent resistivity maps reflect lateral variation of apparent resistivity at a certain depth. In other words, these maps indicate distribution of apparent resistivity in the area against distance of current electrodes. The maximum depth penetration of the AMNB method is 1/3 to 1/4 of the maximum distance of current electrodes [28]. In the case study isoapparent electric resistivity maps were constructed at AB= 100, 200, 300 and 400 m. These maps reflected the lateral variations of the electric resistivity at a depth of about 25, 50, 75 and 100 meters, respectively.

The isoapparent electric resistivity map for AB= 100 m showed the apparent resistivity values in the center, northern and northeastern parts of the study area were lower than elsewhere (Fig. 3a). Because current is conducted electrolytically by the groundwater (in the saturated layers) and by surface contact of minerals (in the dry layers) [29] the low values of apparent resistivity are attributed to the presence of a saturated layer and the high values of apparent resistivity elsewhere to the presence of an unconsolidated and dry layer. The isoapparent electric resistivity map for AB= 200 m indicates the presence of bedrock in the northeast part of area and adjacent mountains and the presence of aquifer elsewhere (Fig. 3b). It showed that the apparent resistivity values in western parts of area were lower than the east. Those in the center were lowest, because sediments grain size decreases towards the center. The isoapparent electric resistivity map for AB= 300 m indicates the presence of an aquifer in the northwestern part of the study area and the presence of bedrock elsewhere (Fig. 3c). High apparent resistivity in the northwestern part of the study area was due to high resistivity of the aquifer because of its coarse grain size. The isoapparent electric resistivity map for AB= 400 m reflects the lateral variation over a horizontal plane at a depth of about 100 meters that indicated the presence of bed rock in the study area (Fig. 3d). The apparent resistivity values of bed rock ranged from 10 to100 ohm-m. Maximum values were recorded in the east. The bedrock was different, with lower apparent resistivity, in the north.

Geoelectrical pseudosections

The geoelectrical pseudosection reflects the apparent resistivity distribution versus electrode spacing values (AB/2). Generally, in the pseudosections of the study area, maximum apparent resistivity values appeared in the upper parts because of the dry alluvium. They decreased toward the middle parts because of the influence of an aquifer then increased with depth because of resistant bed rock. The central parts of the pseudosections were lower than the flanks because of the influence of an aquifer and the coarse grain size dry alluvium along the flanks. In fig. 4, the geoelectrical pseudosection of the profile Z is shown as an example.

Geoelectric sections

In order to have a good understanding of the subsurface geology of the study area geoelectric sections were drawn for each of the profiles. The geoelectric sections reveal the subsurface variation in electrical resistivity and attempts to correlate the geoelectric sequence across the profiles. In this case study, the results of the quantitative interpretation of VES curves are presented as geoelectric sections with a true resistivity distribution, each having 4 interpretable geolelectric layers along the profile (Fig. 5-7).

The near-surface layer had highly variable resistivity ranging from about 3 to 800 ohm-m. The difference in the resistivity values is due to the variation in grain size. Areas with high resistivity values indicated the presence of gravel and sand as top soil, while those with relatively low

resistivity values indicate the presence of clay or intercalation of clay with sand. The thickness of the top soil layer varied. However it often was estimated at less than 15 meters. A second layer (dry alluvium) was thicker than the surface layer and its electrical resistivity was measured typically less than 100 ohm-m. The third geoelectric layer corresponds with a saturated layer, displaying resistivity values of less than 10 ohm-m and depth values of less than 30 meters. The depth of this layer was greater in both the northwest and southeast, and reached 60 meters with an electrical resistivity about 25 ohm-m. This layer was more fine-grained toward the center of the study area. In the center, it had the depth less than 25 meters and a resistivity less than10 ohm-m. The fourth layer was interpreted to be bedrock with low resistivity ranges. In most parts of the area, the resistivity was more than 60 ohm-m corresponding probably to a slate bedrock layer. Where the resistivity value was less than 60 ohm-m corresponding to a shale bedrock layer. The depth of bedrock layer increased toward the center of area. The maximum depth was located in the northwest of region. That was over 100 meters.
Finally the aquifer boundary is determined from the result of quantitative interpretation of VES curves (Fig. 8).

Conclusion

The isoapparent electric resistivity maps showed the apparent resistivity values in the center, northern and northeastern parts of the study area were lower than elsewhere. High values of apparent resistivity dominated the western and eastern parts of the region due to coarse grain talus but in the center, they were lowest due to fine grain character of the alluvial.
Analysis of the geoelectrical pseudosections showed that resistivity values decreased toward the center of the study area due to the decreasing grain size. The eastern and western parts of the study area (flanks of the profiles) had high resistivity. The maximum resistivity values were observed in the surface, whereas minimum values were observed in the saturated zones. Values increased with depth due to presence of bedrock with high resistivity. Low resistivity anomalies were extended to the middle depths of the profiles due to influence of groundwater.
Four major geoelectric layers were identified from the results of qualitative and quantitative interpretation of 596 VES curves in the Curin basin. The first layer was interpreted to be a near-surface layer (top soil) that had a highly variable resistivity ranging from about 3 ohm-m to 800 ohm-m and a thickness of less than 15 meters. The second layer was a dry alluvium layer with a resistivity of less than 100 ohm-m and a thickness of greater than the surface layer. The third geoelectric layer corresponded to a saturated layer and had a resistivity of less than 10 ohm-m with a depth of less than 30 meters in most parts of the area. The fourth layer was interpreted to be bedrock. This layer in most parts of the area was probably slate with a resistivity of more than 60 ohm-m. Elsewhere it had a resistivity of less than 60 ohm-m corresponding to shale.
The boundary of aquifer was determined from quantitative interpretation of the VES data.

References

[1] Kelly WE, Stanislav M, Applied geophysics in hyrogeological and engineering practice. Elsevier 1993.
[2] Ahilan J, Senthil KGR. Identification of aquifer zones by VES method: A case study from Mangalore block, Tamil Nadu, S. India. Archives of Applied Science Research 2011; 3: 414-21.
[3] George NJ, Obianwu VI, Obot IB. Estimation of groundwater reserve in unconfined frequently exploited depth of aquifer using a combined surficial geophysical and laboratory techniques in The Niger Delta, South – South, Nigeria. Advances in Applied Science Research 2011; 2: 163-77.

[4] Emmanuel OJ, Olayinka OO, Oladotun OF. Geoelectric investigation of the groundwater potential of Moniya Area, Ibadan. Journal of Geology and Mining Research 2011; 3: 54-62.
[5] Tahmasbinejad H. Geoelectric investigation of the aquifer characteristics and groundwater potential in Behbahan Azad university farm, Khuzestan province, Iran. Journal of Applied Sciences 2009; 9: 3691-98.
[6] Sikandar P, Bakhsh A, Ali T. Vertical electrical sounding (VES) resistivity survey technique to explore low salinity groundwater for tubewell installation in Chaj Doab. Journal of Agricultural Research 2010; 48: 547-66.
[7] Hodlur GK, Ratnakar D, Sirisha T, Panaskar DB. Resolution of freshwater and saline water aquifers by composite geophysical data analysis methods. Hydrological Sciences Journal 2010; 55: 414-34.
[8] Adeoti L, Alile OM, Uchegbulam O. Geophysical investigation of saline water intrusion into freshwater aquifers: A case study of Oniru, Lagos state. Scientific Research and Essays 2010; 5: 248-59.
[9] Akankpo O, Igboekwe M U. Monitoring groundwater contamination using surface electrical resistivity and geochemical methods. Journal of Water Resource and Protection 2011; 3: 318-324.
[10] Ugwu SA, Nwosu JI. Effect of waste dumps on groundwater in Choba using geophysical method. Journal of Applied Sciences & Environmental Management 2009; 13: 85-9.
[11] Enikanselu PA. Detection and monitoring of Dumpsite-induced groundwater contamination using electrical resistivity method. The pacific journal of science and technology 2008; 9: 254-62.
[12] Cid-Fernández J.A, Araujo PA. VES characterization of a geothermal area in the NW of Spain. EIEAFChe 2007; 6: 2173-77.
[13] El-Qady G. Exploration of a geothermal reservoir using geoelectrical resistivity inversion: case study at Hammam Mousa, Sinai, Egypt. J. Geophys. Eng. 2006; 3: 114-21.
[14] Levi IN. 2D Resistivity survey for groundwater exploration in a hard rock terrain: a case study of Magdas observatory, Unilorin, Nigeria. Asian Journal of Earth Sciences 2011; 4: 46-53.
[15] K'Orowe MO, Nyadawa MO, Singh VS, Ratnakar D. Hydrogeophysical parameter estimation for aquifer characterisation in hard rock environments: a case study from Jangaon sub-watershed, India. Journal of Oceanography and Marine Science 2011; 2: 50–62.
[16] Leo T, Armada CT, Dimalanta GP, et al. Georesistivity signature of crystalline rock in the Romblon Island Group, Philippines. Philippine Journal of Science 2009; 138: 191-204.
[17] Onu NN. Estimates of the relative specific yield of aquifers from geo-electrical sounding data of the coastal plains of southeastern Nigeria. Nigerian Journal of Technology and Education in Nigeria 2003; 8: 69-83.
[18] Ekwe AC, Nnodu IN, Ugwumbah KI, Onwuka OS. Estimation of aquifer hydraulic characteristics of low permeability formation from geosounding data: a case study of Oduma town, Enugu State. Online Journal of Earth Sciences 2010; 4: 19-26.
[19] Egbai JC. Vertical electrical sounding for the determination of aquifer transmissivity. Australian Journal of Basic and Applied Sciences 2011, 5: 1209-14.
[20] Majumdar RK, Das D. Hydrological characterization and estimation of aquifer properties from electrical sounding data in Sagar Island region, South 24 Parganas, West Bengal, India. Asian Journal of Earth Sciences 2011; 4: 60-74.
[21] Taheri TA, Voudouris KS, Salehzadeh M, Mashayekhi H. Hydrogeological framework and estimation of aquifer hydraulic parameters using geoelectrical data: a case study from West Iran. Hydrogeology Journal 2010; 18: 917-29
[22] Amadi AN, Nwawulu CD, Unuevho1 CI, et al. Evaluation of the groundwater potential in

Pompo village, Gidan Kwano, Minna using vertical electrical resistivity sounding. British Journal of Applied Science & Technology 2011; 1: 53-66.
[23] Okolie EC, Atakpo E, Okpikoro FE. Application of linear Schlumberge array in delineation of formation strata and groundwater
distribution in Ifon Ondo State, Nigeria. Int. J. Phy. Sci. 2010; 5: 642-650.
[24] Danielsen J, Dahlin T, Owen R, Mangeya P, Auken E. Geophysical and hydrogeologic investigation of groundwater in the Karoo stratigraphic sequence at Sawmills in northern Matabeleland, Zimbabwe: a case history. Hydrogeology Journal 2007; 15: 945-60.
[25] Yusuf SN, Joseph MV, Alkali SC, Kuku AY. Determination of porous zones using vertical electrical sounding data from basement rocks of Hussara, Askira UBA, North-eastern Nigeria. Ozean Journal of Applied Sciences 2011; 4: 183-189.
[26] Frohlich RK, Parke CD. The electrical resistivity of vadose zone–field survey. Groundwater 1989; 27: 524-530.
[27] Orellana E, Mooney HM. Master tables and curves for electrical sounding over layered structure interciencia. Madrid: 1966.
[28] Frohlich RK, Fisher JJ, Summerly E. Electric-hydraulic conductivity correlation in fractured crystalline bedrock: Central Landfill, Rhode Island. USA. J. Applied Geophysics 1996; 35:249-59.
[29] Zohdy AAR, Eaton GP, Mabey DR. Application of surface geophysics to ground-water investigations. 1[nd] edn, U.S. Geol. Surv. Techn. Water Res. Invest 1974.

Figures:

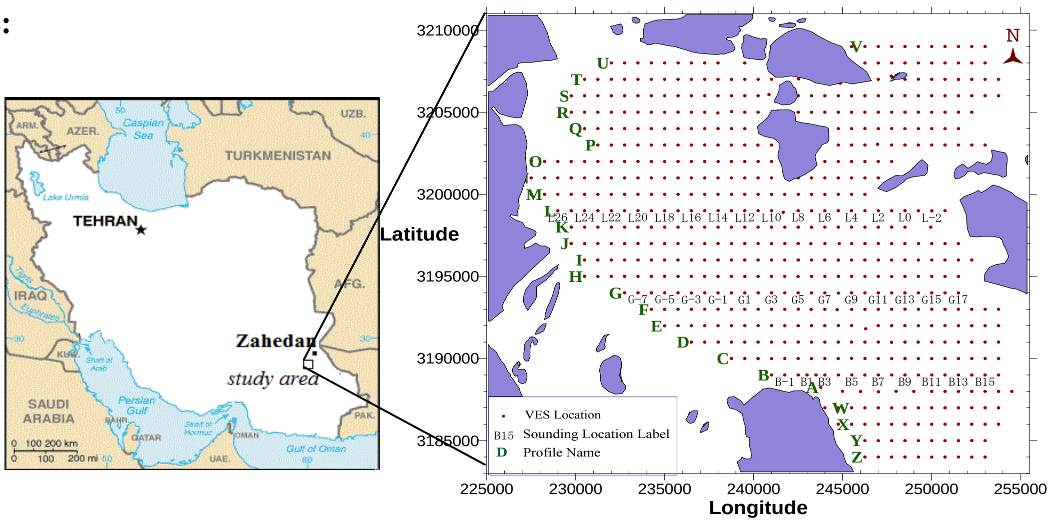

Fig. 1: Location map of the study area showing VES locations.

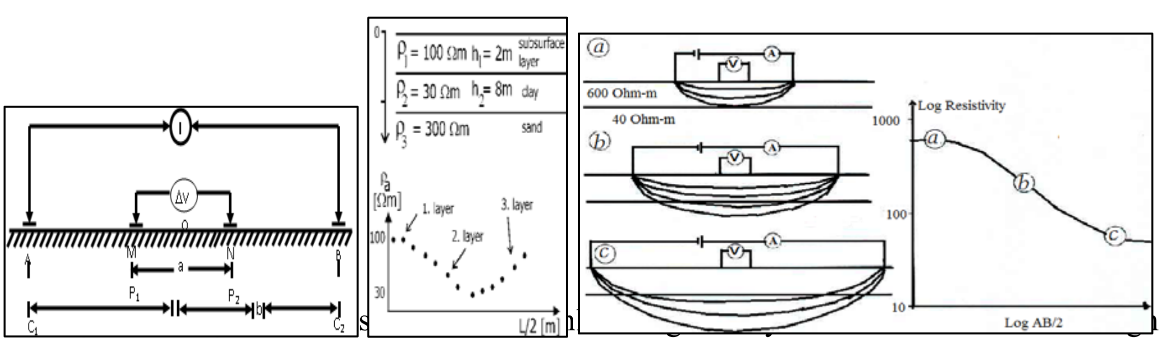

electrodes A and B, and voltage readings are made with electrodes M and N, (b)A Schlumberger sounding curve in a simple three-layer system. The apparent resistivity is plotted versus the AB/2, (c) As the distance between the current electrodes is increased, so the depth to which the current penetrates is increased.

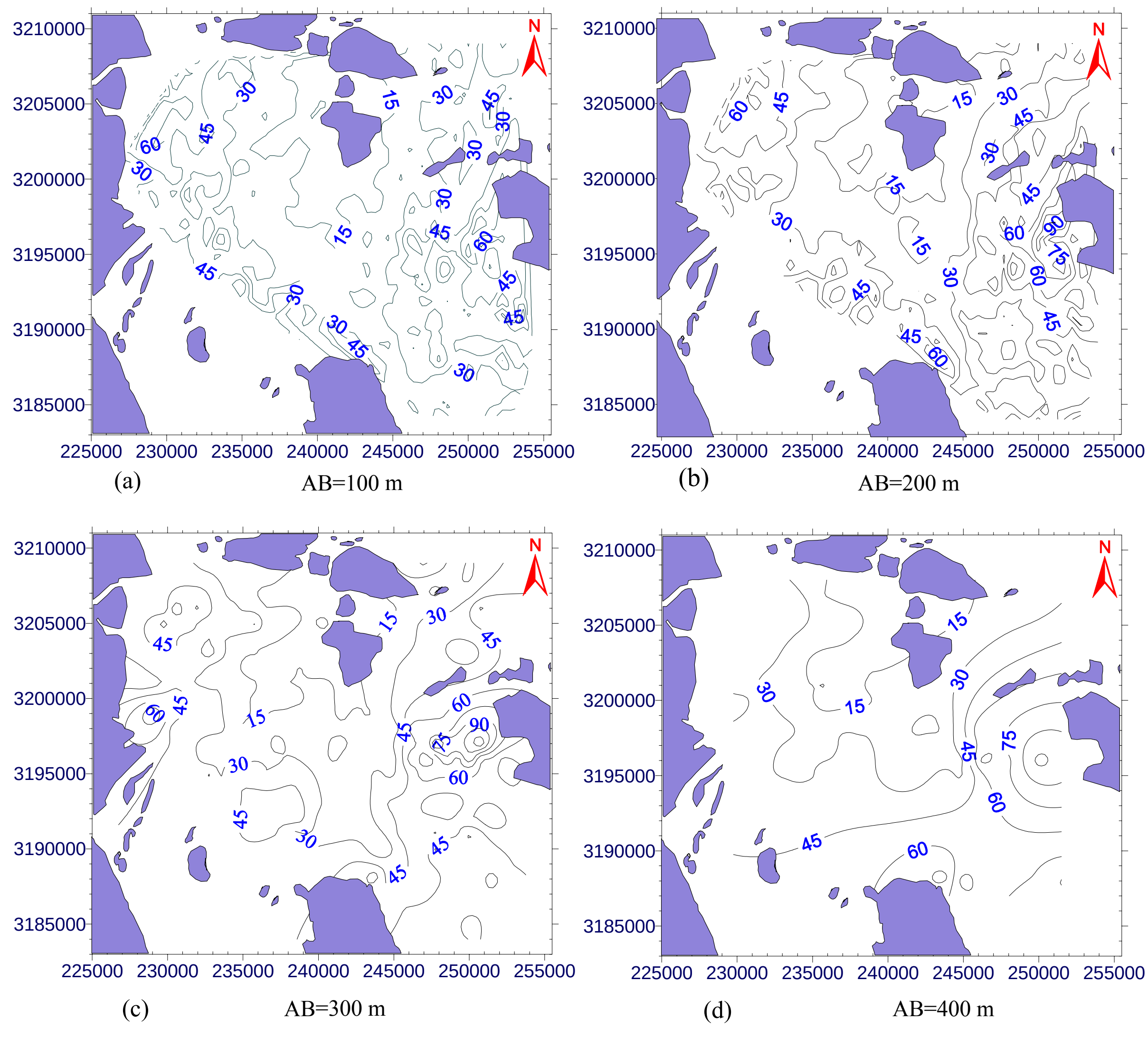

Fig. 3: Isoapparent resistivity map for AB=100 m(a), 200 m(b), 300 m(c) and 400 m(d) showing the lateral variations of the resistivity at a depth of about 25 m(a), 50 m(b), 75 m(c) and 100 m(d).

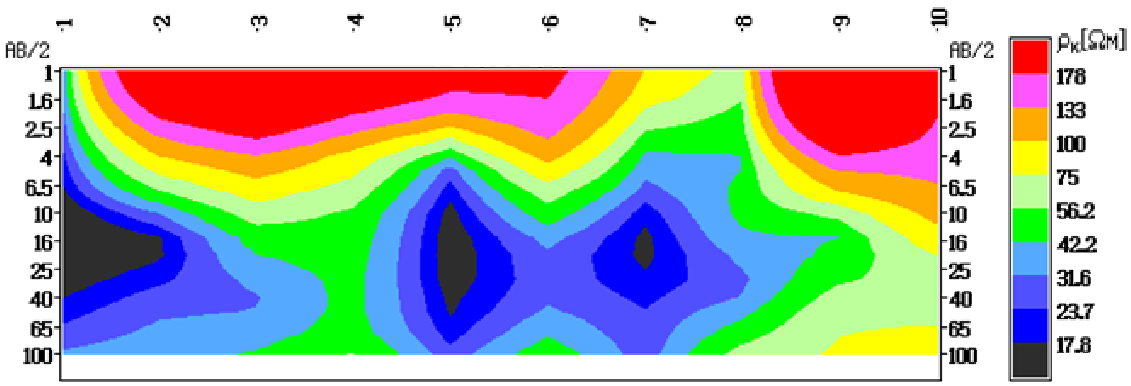

Fig. 4: Pseudosection of the profile Z.

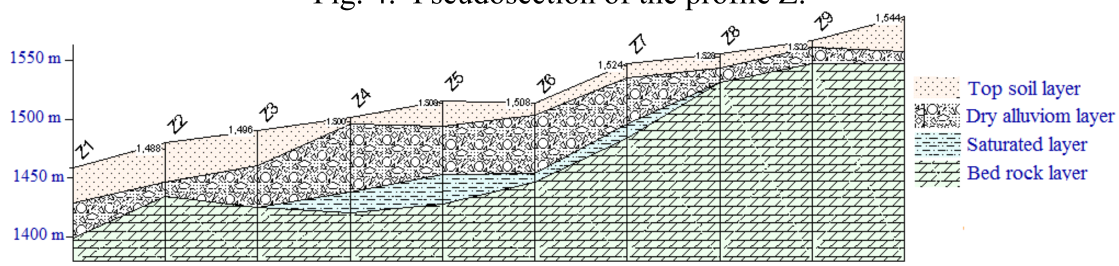

Fig. 5: Geoelectric section of profile Z.

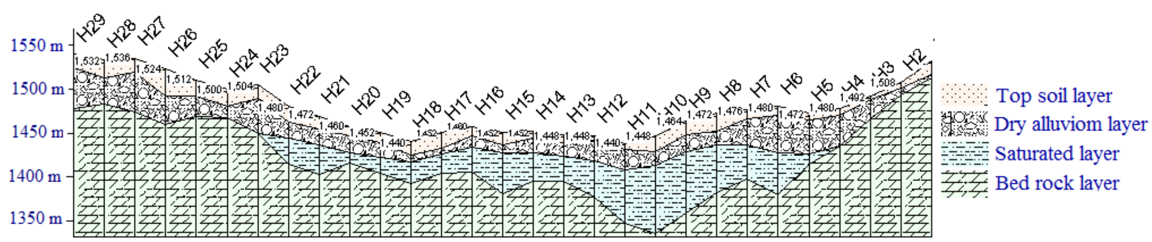

Fig. 6: Geoelectric section of profile H.

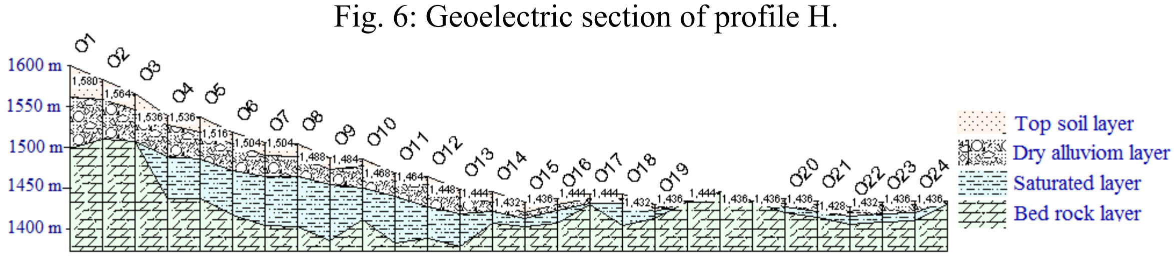

Fig. 7: Geoelectric section of profile O.

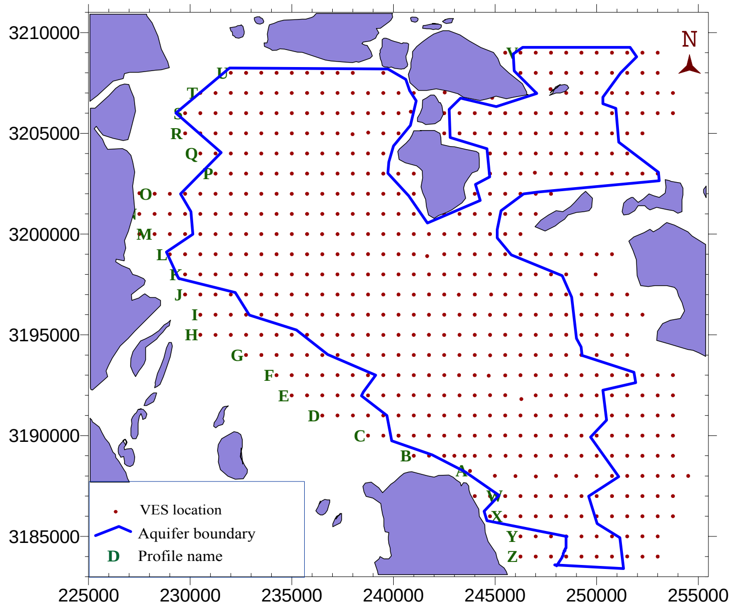

Fig. 8: Aquifer boundary map.